# Monte Carlo Calculations in the Isothermal–Isobaric Ensemble. 2. Dilute Aqueous Solution of Methane[1]

**John C. Owicki[2a] and Harold A. Scheraga*[2b]**

*Contribution from the Department of Chemistry, Cornell University, Ithaca, New York 14853.* *Received February 10, 1977*

**Abstract:** A Monte Carlo simulation of a dilute aqueous solution of methane is carried out in the isothermal–isobaric ensemble at 298 K and atmospheric pressure. The methane–water pair potential energy function developed for the calculations was parametrized to fit an ab initio SCF energy hypersurface. The model satisfactorily reproduces the experimental values of the solvation partial molar energy and volume. Interactions between water molecules in the solvation shell are more stable and more sharply distributed than those in the bulk liquid. The computed methane coordination number is similar to the number of water molecules in the polyhedral cages in the methane clathrate.

## I. Introduction

Aqueous solutions of nonpolar nonelectrolytes are of great interest in biophysical chemistry as model systems for the study of the factors responsible for the hydrophobic interaction.[3] Of the commonly studied aqueous solutions, these are simultaneously among the most elementary and the most complicated. Their simplicity derives from the fact that the solute–solvent interaction does not include any strong attractive forces; instead, it is primarily an excluded-volume effect. In the absence of such attractions, however, the structure and thermodynamic properties of the solutions appear to be dominated by subtle shifts in the hydrogen-bonding interactions among the water molecules surrounding the solute.

When a nonpolar nonelectrolyte is transferred from the gas phase to water, the changes in several thermodynamic properties differ in characteristic ways from the corresponding changes for the same process in most nonaqueous solvents. In the aqueous system, the enthalpy change is more negative[4] and the increase in the volume of the solution is smaller. The larger relative decrease in entropy and increase in heat capacity are striking. Many structural theories have been proposed to account for these basic thermodynamic observations,[3,5] most being based on the hypothesis by Frank and Evans[6] that a nonpolar solute increases the degree of hydrogen bonding (i.e., the "icelikeness") of water molecules in the solvation shell. Nonpolar gases form (crystalline) clathrate hydrates in which each guest gas molecule is surrounded by a polyhedral cage in the lattice of host water molecules,[7] and several workers[3,5] have developed the idea that the solvation shell in solution resembles these cages, at least in part.

In the first paper in this series,[8] hereafter referred to as part 1, we investigated the structure and thermodynamic properties of liquid water by Monte Carlo (MC) computations in the isothermal–isobaric or $(T,P,N)$ ensemble. This paper extends these calculations to a dilute aqueous solution of methane. Part of its purpose is to determine how accurately a model system can reproduce experimental findings, using fairly realistic pair potentials. Perhaps more important, though, is the calculation of structural and energetic quantities which would be difficult or impossible to obtain experimentally.

In section II we discuss and define the statistical-mechanical functions which will be studied. Section III presents the MC technique, and section IV describes the pair potential energy functions used. The theoretical results are given and discussed in section V. Finally, a summary of our findings and the most important conclusions to be drawn comprise section VI.

## II. Statistical Mechanics

**A. Introduction.** This section extends the statistical-mechanical notation and formalism of part 1 to dilute aqueous solutions. For additional definitions and greater detail about water–water interactions, the reader is directed to section II of part 1.

**B. Dilute Aqueous Solutions of Methane.** The system of interest is $N$ water molecules and one methane molecule in the $(T,P,N)$ ensemble. When it is necessary to distinguish properties of this system from those of the pure liquid ($N$ water molecules), we use the subscripts "$N + CH_4$" and "$N$," respectively.

If the molecular coordinates of methane are denoted as $\mathbf{X}_{CH_4}$, the pair interaction energy (see section IV) between the methane and water molecule $i$ is $U(\mathbf{X}_{CH_4},\mathbf{X}_i)$. The binding energy of the methane to the solvent is

$$B_{CH_4}(\mathbf{X}_{CH_4},\mathbf{X}^N) \equiv \sum_i U(\mathbf{X}_{CH_4},\mathbf{X}_i) \tag{1}$$

The potential energy of the system then is

$$U_{N+CH_4}(\mathbf{X}_{CH_4},\mathbf{X}^N) \equiv U_N(\mathbf{X}^N) + B_{CH_4}(\mathbf{X}_{CH_4},\mathbf{X}^N) \tag{2}$$

$U_{N+CH_4}$ is the energy to be used in the Boltzmann factor for ensemble averages, etc., of the solution.

**C. Partial Molar Quantities.** For a mechanical property $F(\mathbf{X}^N,V)$, the partial molar quantity $\Delta F$ can be defined as the change in the ensemble-average value of $F$ on the addition of one molecule of solute to the system.[9]

$$\Delta F \equiv \langle F_{N+CH_4} \rangle - \langle F_N \rangle \tag{3}$$

$\Delta F$ is a function of $N$. As $N \to \infty$, however, $\Delta F \to \Delta F^\circ$, the infinite-dilution value. The two most important partial molar quantities for the purposes of this paper are $\Delta U^\circ$ and $\Delta V^\circ$.

**D. Shell vs. Bulk Molecules.** We shall distinguish between two classes of solvent molecules. Those which are in the first solvation shell of the solute are called shell molecules. Solvent molecules in the solution are called bulk molecules, provided that they are sufficiently far from the solute not to be perturbed by its presence; also, those in the pure liquid are called bulk molecules. More precisely, shell molecules are those whose centers (oxygen nuclei) lie within some fixed distance $\hat{R}$ of the center of the solute (the carbon nucleus). $\hat{R}$ is chosen to include the first peak of the solute–solvent radial distribution function $g_{CO}$.

A good way of studying solutions, especially structural and energetic effects therein, is to compare the average properties of shell and bulk (solvent) molecules. Of particular interest are the probability distribution functions (PDF's) for the binding energies ($P_B$; this does not include interactions with the solute) and pair interaction energies between nearest neighbors ($P_{UNN}$). Two water molecules are considered to be nearest neighbors when their oxygen nuclei are separated by less than 3.6 Å; this distance is the position of the first minimum in the

oxygen–oxygen radial distribution function for bulk water in this model.[8]

**E. Radial Distribution Functions (RDF's).** There are four solute–solvent atom–atom RDF's ($g_{CO}$, $g_{CH}$, $g_{HO}$, $g_{HH}$), which contain a great deal of information about the structure of the solvation shells of the solute. The integrated form, $N_{CO}(R)$, gives the number of water molecules (i.e., oxygens) within a sphere of radius $R$ about the methane carbon.

## III. Monte Carlo Procedures

**A. General.** Since experiments are carried out at constant pressure and since volume effects are of interest, it is advantageous to perform calculations under conditions where the volume is allowed to fluctuate. Our MC computations, therefore, were carried out in the $(T,P,N)$ ensemble as described in part 1. Modifications of the procedure for calculations on solutions are outlined in this section.

The conditions chosen were the same as for chain II in part 1, viz., $T$ = 298 K, $P$ = 1 atm, and $N$ = 100 water molecules, with face-centered-cubic periodic boundary conditions (PBC). Rather than select a random starting configuration, we inserted a methane molecule in a cavity (with a radius of ~3.5 Å, and containing no oxygens) which we had located in the final configuration from the computation (chain II) for the pure liquid. The coordinate system then was translated to place the carbon nucleus at the center of the base cell. The solute molecule remained fixed at the origin throughout the computation. Holding the methane stationary does not make the calculation inapplicable to the physical case of a mobile methane; we merely have chosen to fix the coordinate system on the solute. Several hundred thousand steps were discarded for equilibration prior to the computation of ensemble averages over an additional 674 000 steps.

To facilitate the collection of long-range RDF data, the cutoff distance for evaluating the methane–water pair energy was taken as 8.9 Å, compared to 6.35 Å for the water–water pair energy. A dispersion correction for the cutoff of the solute–solvent potential, made by analogy to eq 28 in part 1, added only about −0.22 kcal/mol to $\overline{U_{N+CH_4}}$ and $\overline{B_{CH_4}}$. No long-range dipole–dipole correction was required because the dipole moment of methane is zero.

**B. Preferential Sampling Near the Solute.** The most interesting region of the solution is that near the solute, where solute–solvent interactions are strongest. Hence, it is useful to sample this area more thoroughly than outlying regions, by perturbing molecules close to the solute more often than those which are far away. The "close" molecules were identified with the shell molecules of section IID, and the limit of the first hydration shell was defined to be $\hat{R}$ = 5.5 Å, based on preliminary calculations.[10] An algorithm which we have described elsewhere[11] was used for the preferential sampling.

Initially, upon insertion of the methane, almost all of the sampling was concentrated (intentionally) on the shell molecules. In subsequent stages of the equilibration, the perturbations were spread somewhat more evenly and, during the part of the chain used for averaging, the sampling of shell molecules was enhanced about twofold over normal.

**C. Periodic Boundary Conditions for the Solution, and Preliminary Calculations.** PBC are less satisfactory for modeling solutions than for modeling pure liquids. Although the present system is supposed to represent infinite dilution, molecules in the base cell are influenced by the solutes centered in the surrounding cells. This is an indirect interaction, since no pair energies involving these external solute molecules are evaluated; the indirect interaction can be visualized as an overlap of the outer hydration shells of adjacent solutes. One hopes that, with a short-range solute–solvent interaction, this will be a small perturbation for manageably small values of $N$.[12]

In a preliminary MC calculation, conducted as above but with $N$ = 64 and simple-cubic PBC, we found that this interaction was not small. The mean separation of adjacent solute molecules (13.8 Å) was not sufficient for the formation of the second solvation shell ($R_{CO}$ = 6.5–7.5 Å, based on calculated radial distribution functions). Consequently, the introduction of the methane caused a disruption of hydrogen bonds throughout the solution, and resulted in a calculated value of $\Delta U^\circ$ = +23 ± 7 kcal/mol, compared to the experimental value[13] of −2.6 kcal/mol. Increasing $N$ to 100 and changing the PBC to face-centered-cubic added 4.0 Å to the methane–methane separation, which is equivalent to between one and two layers of water molecules. This improved the calculated value of $\Delta U^\circ$ and seemed more realistic, judging from the $g_{CO}$ curve. The results of this computation are presented in section V.

## IV. Potential Energy Functions

**A. Methane–Water Pair Potential.** Clementi and co-workers[14] have demonstrated that realistic intermolecular potential energy functions can be constructed by adjusting the parameters of an empirical function to obtain the best least-squares fit to a set of points on an ab initio SCF quantum-mechanical potential energy hypersurface for the system. We have used this technique to derive a methane–water potential based on an ab initio study by Ungemach and Schaefer.[15]

Twenty-eight configurations were selected from the ab initio potential curves in Figure 3 of ref 15. These were composed of five types of orientations of the molecules, with $R_{CO}$ between 3.1 and 5.5 Å, and with energies between −0.46 and +2.23 kcal/mol. This set of fitting points was chosen to contain neither very high-energy configurations nor configurations with large intermolecular distances. The former are difficult to fit accurately and are unimportant in calculations on liquids, while the latter (which are near zero energy) are too easy to fit with a wide range of parameters and thus are not very useful for determining the parameters of the potential.

The functional form that we chose is presented in Table I and Figure 1, along with the best-fit values of the nine adjustable parameters. The experimental geometries were used, viz., $R_{CH}$ = 1.094 Å,[16] $R_{OH}$ = 0.9572 Å, and ∠HOH = 104.52°.[17] "M" is the site of the negative charge in the CI water potential,[14] and $R_{OM}$ = 0.2676 Å. Terms proportional to $r^{-1}$ and $r^{-12}$ act between nuclei, and there are $r^{-6}$ interactions between the "M" point and the hydrogen nuclei of methane. The $r^{-1}$ terms are similar to Coulombic interactions, but they are more general in that they introduce four free $a_{kl}$ parameters rather than one (a product of the partial charges on the pairs of nuclei).[18] Since this potential is simply an analytical fitting function, its individual terms should not be given a physical interpretation.

The root mean square deviation of the potential from the ab initio points is 0.08 kcal/mol. The most important error (and it is not serious) is a tendency for the empirical energies to be ~0.1 kcal/mol high in the lowest energy configurations. It is useful to know the range of interaction energies possible for a given $R_{CO}$. Therefore, in Figure 2, we have plotted the minimum and maximum pair interaction energies as a function of the C···O separation. The *maximum* curve corresponds to orientations where C–H···H–O are collinear. The orientations making up the *minimum* curve are more varied, but the global minimum, $U$ = −0.42 kcal/mol at $R_{CO}$ = 3.58 Å, is shown in Figure 3. Also shown are three other favorable configurations. For $R_{CO} \lesssim 4.2$ Å, molecular structure becomes important, in the sense that there are orientations that differ in energy by $> kT$ (for $T \sim 300$ K).

The question arises as to how realistic the potential is. As a result of the fitting constraints and the omission of correlation effects in the ab initio calculations,[15] the attractive wells

**Table I.** Empirical Potential for Methane-Water Interactions[a]

| $a_{kl}$, kcal Å/mol | | | $b_{kl}$, kcal Å$^{12}$/mol | | |
|---|---|---|---|---|---|
| $k$ | $l = 1$ | $l = 2,3$ | $k$ | $l = 1$ | $l = 2,3$ |
| 1 | 166.428 | −80.9846 | 1 | $1.63977 \times 10^6$ | $3.56973 \times 10^4$ |
| 2,3,4,5 | −41.8154 | 20.3510 | 2,3,4,5 | 6683.91 | 975.403 |

[a] $U = \Sigma_{k=1}^{5} \Sigma_{l=1}^{3} (a_{kl}/r_{kl} + b_{kl}/r_{kl}^{12}) - \Sigma_{k=2}^{5} c/r_{k4}^{6}$, with $c$ = 119.598 kcal Å$^2$/mol. The first subscript ($k$) refers to points on the methane molecule, and the second ($l$) refers to points on the water molecule. The points are numbered as in Figure 1.

probably are not deep enough. This is compensated for partially by the fact that the ab initio $CH_4$–$H_2O$ energies probably are below those which would be obtained in the Hartree–Fock limit.[15] The orientational dependence of the short-range repulsions is complicated, and this potential provides a significant improvement over a simplified orientation-averaged model (e.g., an interaction solely between C and O[19]).

**B. Water–Water Pair Potential.** As in part 1, water–water interactions were modeled with the CI potential.[14]

## V. Results and Discussion

**A. $\Delta U^\circ$ and $\Delta V^\circ$.** In calculating these partial molar quantities, the values of the potential energy and volume for the pure liquid were taken from part 1. For a comparison of these bulk values with experiment, the reader should consult Table III, section VIIB, and section VIIC of that paper. The standard errors of the calculated partial molar quantities are the square roots of the sums of the squares of the component standard errors. For the partial molar energy, we obtained

$$\overline{U_{N+CH_4}} = -918 \pm 7 \text{ kcal/mol}$$

$$\overline{U_N} = -907 \pm 13 \text{ kcal/mol}$$

$$\Delta U^\circ = -11 \pm 15 \text{ kcal/mol}$$

$$\text{exptl}[13]\ \Delta U^\circ = -2.6 \text{ kcal/mol}$$

Likewise,

$$\overline{V_{N+CH_4}} = 2406 \pm 30 \text{ cm}^3\text{/mol}$$

$$\overline{V_N} = 2381 \pm 16 \text{ cm}^3\text{/mol}$$

$$\Delta V^\circ = 25 \pm 34 \text{ cm}^3\text{/mol}$$

$$\text{exptl}[20]\ \Delta V^\circ = 37 \text{ cm}^3\text{/mol}$$

Thus, in both cases the experimental values lie within the calculated ranges. However, the errors are so large that the signs of the calculated quantities could be reversed. The reason clearly is that small differences are being taken between large numbers, with consequent magnification of the relative error. For example, in order to determine $\Delta U^\circ$ to within ±1 kcal/mol, the percent error in $\overline{U_{N+CH_4}}$ or $\overline{U_N}$ must be $\lesssim 7/N$, assuming that these errors are equal and independent. With $N$ = 64, the allowed error is ±0.12%, and for $N$ = 100 it is ±0.07%. While MC and molecular dynamics calculations on simple liquids may attain this precision, it is our opinion that it would require prohibitively long computations to obtain the same precision for an aqueous system, with typical contemporary computing capabilities. We, therefore, suggest that thought be given to the development of techniques which are inherently differential or which produce a high correlation between the errors in the calculations on the solution and on the pure liquid.

The precision in our calculated heat capacities, compressibilities, and expansibilities is not high enough to justify the calculation of the associated partial molar quantities.

Dashevsky and Sarkisov[21] performed extensive MC calculations on methane in the ($T$,$V$,$N$) ensemble with $N$ = 64. Their results for $\Delta U^\circ$, $\Delta A^\circ$ (where $A$ is the Helmholtz free energy), and $\Delta S^\circ$ were in good agreement with experiment. While we have found much worthwhile information in their paper, we feel strongly that, aside from their use of such a small value of $N$, the technique that they used to determine free energies (and therefore entropies) was computationally ill-conditioned and hence unreliable. Our objections to the use of this method for the pure liquid[19] can be found in section VIII of part 1. The addition of the solute and the necessity to subtract in forming the partial molar free energy are unlikely to improve matters.

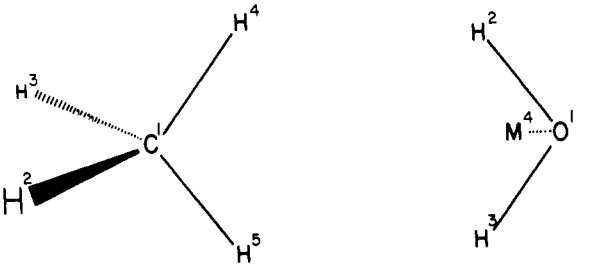


**Figure 1.** Numbering of points on molecules for methane–water pair potential energy function. The "M" point is on the $C_2$ axis of the water molecule.

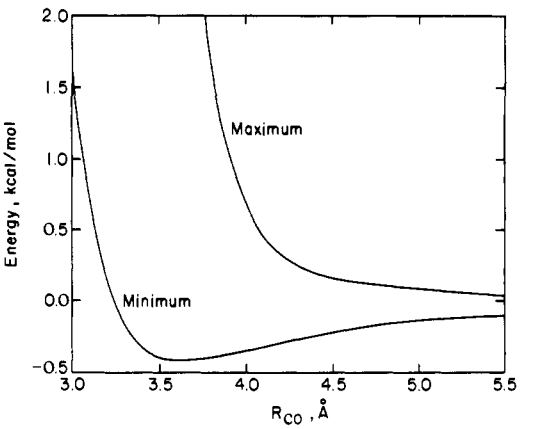


**Figure 2.** Methane–water potential energy. For each value of $R_{CO}$, the points on the curves represent the minimum and maximum energies over all orientations of the molecules.

**B. Solute–Solvent Radial Distribution Functions.** The calculated $g_{CO}$ curve is presented in Figure 4 along with the running coordination number $N_{CO}$; $g_{CH}$, $g_{HO}$, and $g_{HH}$ are given in Figure 5. The experimental determination of these functions (e.g., by diffraction techniques) is an extremely difficult technical problem which has not yet been solved.

Probably the most important single observation to be made is that the first hydration shell is broad (from $R_{CO} \sim 3.1$ to 6.0 Å) and contains ~23 water molecules. For comparison, in this model the bulk water–water first hydration shell extends from $R_{OO} \sim 2.4$–3.6 Å and contains ~four water molecules. This will be discussed more fully in section VD.

It is difficult to interpret the radial distribution functions uniquely in terms of preferred molecular orientations. However, some general conclusions can be made. There are sig-

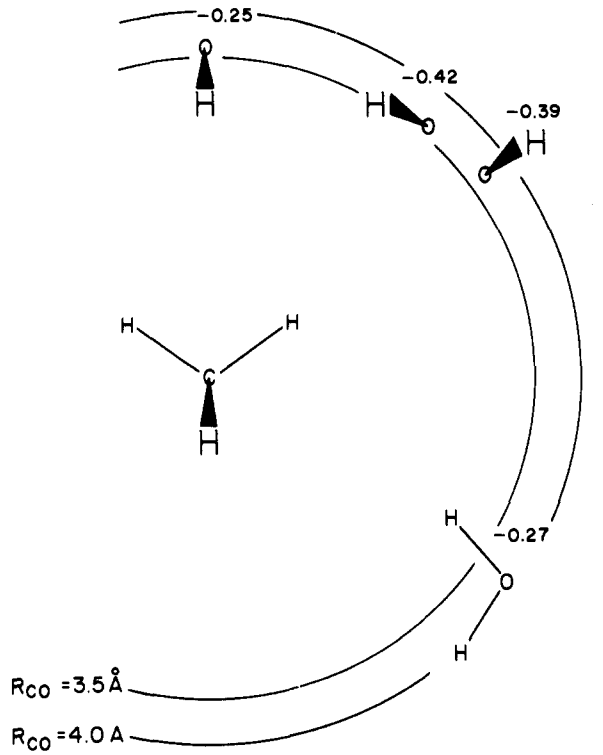


**Figure 3.** Four selected low energy methane–water configurations. Each configuration is labeled with its energy in kcal/mol; the one marked −0.42 is the global minimum on the empirical potential energy hypersurface. The wedge-shaped bonds mask mirror-symmetric bonds below the plane of the paper.

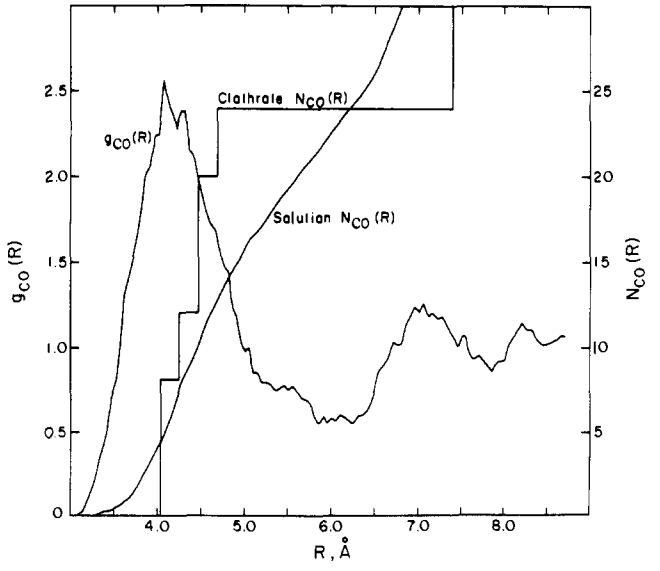


**Figure 4.** Calculated carbon–oxygen radial distribution function $g_{CO}$ and running coordination number $N_{CO}$. Also included is idealized $N_{CO}$ for methane in a clathrate cage; see section VD.

nificant CO and CH correlations at least out through the second hydration shell. The HO and HH correlations are weaker. Judging from the peaks in the $g_{CO}$ and $g_{CH}$ curves, in the first shell there is some preference for the water hydrogens to be closer than the oxygens to the center of the methane. That this situation is reversed in the second shell is consistent with hydrogen bonding between the shells.

Two intriguing features of the calculated RDF's are the valleys in $g_{CO}$ near 7.8 Å and in $g_{CH}$ near 4.7 Å. Although they are above the ~10% noise level in these functions, they may be artifacts. This is related to a general problem that we have

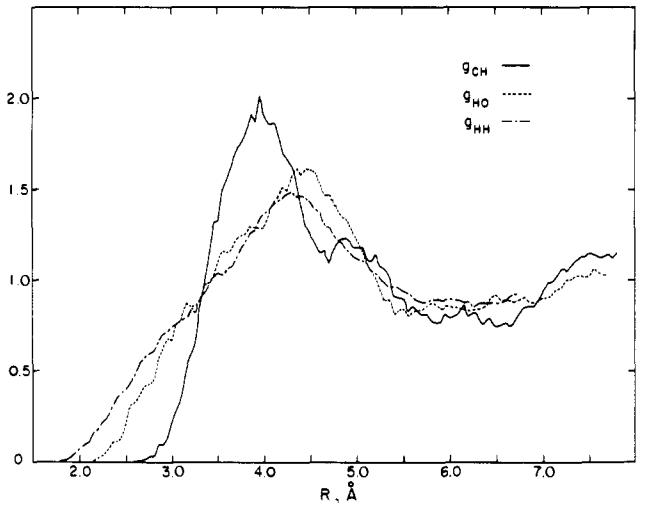


**Figure 5.** Calculated carbon–hydrogen, hydrogen–oxygen, and hydrogen–hydrogen solute–solvent radial distribution functions $g_{CH}$, $g_{HO}$, and $g_{HH}$.

found in doing MC calculations on aqueous systems. In the pure liquid, the MC calculation of a quantity such as an RDF can be thought of as occurring in two steps: first, an averaging over the environment of *each* of the $N$ molecules during the course of the Markov chain; second, a subsequent averaging over the results for all $N$ molecules, since they are in principle indistinguishable. It has been our experience that the orientational forces in water are so strong that atypical structural features in the environment of a given molecule may persist to a measurable extent throughout the calculation. Averaging over all the molecules removes this quasi-ergodic problem, but no such averaging can be done for a single solute.[22] The most obvious remedy in such cases is to do multiple calculations from different initial configurations; this is, of course, very expensive. In the absence of such a calculation, it is not possible to say for certain whether the valleys near 7.8 and 4.7 Å are artifacts.

**C. Energy Probability Distribution Functions.** If nonpolar solutes increase the "structure" of the nearby water molecules, there should be a strengthening of the solvent–solvent interactions within and around the solvation shell. That something like this is true in the present model is suggested by the fact that the calculated $\Delta U°$ (−11 ± 15 kcal/mol) probably is more negative than the calculated mean methane binding energy ($\overline{B_{CH_4}}$ = −0.87 ± 0.09 kcal/mol). The energy PDF's, $P_{UNN}$ and $P_B$, support this conclusion and add much more detail to the picture.

$P_{UNN}$ was calculated for three sets of conditions on the tabulated nearest-neighbor water pairs: (1) when both were bulk molecules (taken from part 1), (2) when one was a shell molecule and one lay outside the shell, and (3) when both were shell molecules. These PDF's probed the distribution of interactions of adjacent water molecules which were far from the solute, across the first hydration shell boundary, and within the shell, respectively. As can be seen from the plots in Figure 6, the differences are clear but not dramatic. The methane both sharpens the distribution and shifts it toward lower energies, and the size of this effect diminishes with increasing distance from the methane. This also can be seen by calculating the means of the distributions, giving the mean nearest-neighbor energies, $\overline{U_{NN}}$:

| | |
|---|---|
| bulk | −3.52 ± 0.07 kcal/mol |
| across shell boundary | −3.63 ± 0.05 kcal/mol |
| within shell | −4.02 ± 0.16 kcal/mol |

Similarly, the distributions of solvent–solvent binding

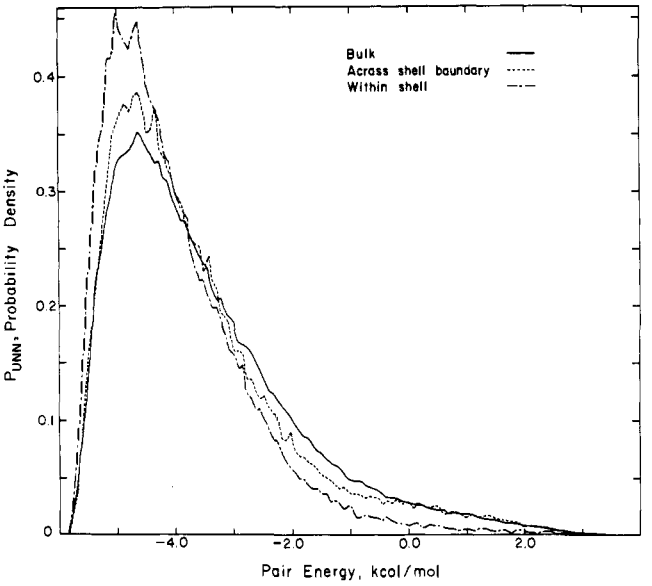


**Figure 6.** Probability distribution functions $P_{UNN}$ for pair energies between nearest-neighbor water molecules in three environments.

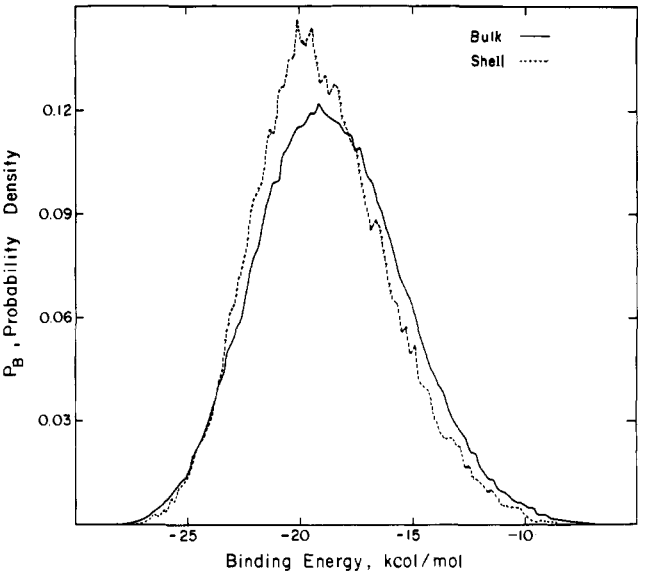


**Figure 7.** Probability distribution functions $P_B$ for solvent-solvent binding energies, for water molecules in two environments.

energies, $P_B$, for bulk and shell molecules can be compared. This is done in Figure 7, and again the distribution of shell molecule energies is sharper and more negative than that for bulk molecules. The mean binding energies, $\bar{B}$, are:

| | |
|---|---|
| bulk molecules | $-18.14 \pm 0.26$ kcal/mol |
| shell molecules | $-18.82 \pm 0.56$ kcal/mol |
| $\Delta$ (shell-bulk) | $-0.68 \pm 0.62$ kcal/mol |

The above difference is less than might have been expected on the basis of the nearest-neighbor energy results. This might be caused by less favorable second-neighbor interactions involving shell molecules. Another effect which certainly accounts for part of this is the weak interaction between the methane and shell molecules, which we computed to be only $-0.027 \pm 0.004$ kcal/mol of pair interaction; replacement of the methane by a water molecule would be energetically favorable with respect to this quantity.

**D. Comparison with Clathrate.** Although the disorder in the first solvation shell is too great for it to be considered as a true clathrate cage (or any other crystalline arrangement), there is at least one striking similarity, viz., the calculated coordination number, 23, is between the sizes of the two clathrate cages which methane is known to occupy,[7] 20 and 24. Included in Figure 4 is the idealized $N_{CO}$ curve, based on a methane immobilized at the center of one of the larger cages. In a more realistic representation, with the methane allowed to move inside the cage, the curve would be more smeared out and would resemble the solution $N_{CO}$ curve somewhat more closely. It should be noted that the distance between the first and second peaks of the solution $g_{CO}$ curve corresponds closely to the separation between clathrate cage ($H_2O$) molecules and their ($H_2O$) neighbors outside the cage. Adding to these arguments the strengthened and sharpened solvent-solvent interactions in the hydration shell, one easily can see the qualitative reasonableness of clathrate models for the solvation of small nonpolar molecules.

## VI. Summary and Conclusions

This paper has reported a Monte Carlo (MC) simulation of a dilute aqueous solution of methane in the isothermal-isobaric ensemble, using an empirical methane-water pair potential energy function fit to an ab initio SCF energy hypersurface. Within very large standard errors, the calculated solute partial molar energy and volume agree with the experimental values.

The four atom-atom solute-solvent radial distribution functions have been computed, with the finding that the first solvation shell is broad and contains ~23 water molecules. Probability distribution functions for nearest-neighbor energies and binding energies indicate that the environments of molecules in the shell are characterized by lower, more sharply distributed energies than are the environments of bulk molecules. These results support the concept that nonpolar solutes increase the degree of hydrogen bonding or structure in their hydration shells. In the present MC model, such ordering is not strictly equivalent to the formation of a clathrate cage, but strong resemblances do exist—particularly between the calculated coordination number of methane and the sizes of the cages in the methane clathrate.

We plan to do a more complete geometrical analysis of the solvation shell, based on configurations which were saved on magnetic tape after each 10 000 steps in the MC chain. Although we believe that this study has been successful, there is a need for the development of improved computational techniques to deal with what amounts to the low signal to noise ratio in MC (or MD) calculations on dilute solutions.

## References and Notes

(1) This work was supported by research grants from the National Science Foundation (PCM-75-08691) and from the National Institute of General Medical Sciences of the National Institutes of Health, U.S. Public Health Service (GM-14312).
(2) (a) NIH Trainee. (b) To whom requests for reprints should be addressed.
(3) (a) G. Nemethy and H. A. Scheraga, *J. Chem. Phys.*, **36**, 3401 (1962); (b) *J. Phys. Chem.*, **66**, 1773 (1962); **67**, 2888 (1963).
(4) Except for the larger hydrocarbons. For a review of the thermodynamic properties of these solutions, see F. Franks and D. S. Reid in "Water, a Comprehensive Treatise", Vol. II, F. Franks, Ed., Plenum Press, New York, N.Y., 1973, Chapter 5.
(5) These are reviewed by F. Franks in ref 4, Chapter 1.
(6) H. S. Frank and M. W. Evans, *J. Chem. Phys.*, **13**, 507 (1945).
(7) D. W. Davidson, in ref 4, Chapter 3.
(8) J. C. Owicki and H. A. Scheraga, *J. Am. Chem. Soc.*, preceding paper in this issue.
(9) Thermodynamically, of course, partial molar quantities are derivatives. However, the number of solute molecules becomes a discrete variable at the microscopic level; these quantities then can be expressed as finite differences upon the addition of one solute molecule.
(10) As it turned out in the main calculation, the first minimum in $g_{CO}$ occurred at $R = 6.0$ Å instead of at 5.5 Å, but the exact value chosen is not particularly important, since the parameter $\bar{R}$ affects the sampling routine, but not the physics of the problem. The larger value was used to define the limit of the solvation shell only in the computation of the coordination number. The smaller value was used to define "shell" molecules (section IID), but this should make no qualitative difference in the results reported in section VC.

(11) J. C. Owicki and H. A. Scheraga, *Chem. Phys. Lett.*, **47**, 600 (1977).
(12) An alternative to PBC is to enclose the solute and $N$ solvent molecules in a cavity in a dielectric continuum. See, e.g., D. L. Beveridge and G. W. Schnuelle, *J. Phys. Chem.*, **78**, 2064 (1974). This introduces problems of its own, however, such as strong nonphysical orientational forces on water molecules near the surface of the cavity (J. C. Owicki and H. A. Scheraga, unpublished results).
(13) M. Yaacobi and A. Ben-Naim, *J. Phys. Chem.*, **78**, 175 (1974).
(14) (a) O. Matsuoka, E. Clementi, and M. Yoshimine, *J. Chem. Phys.*, **64**, 1351 (1976); (b) G. C. Lie, E. Clementi, and M. Yoshimine, *ibid.*, **64**, 2314 (1976).
(15) S. R. Ungemach and H. F. Schaefer III, *J. Am. Chem. Soc.*, **96**, 7898 (1974). The experimental geometries and a double-$\zeta$ basis set of contracted Gaussian functions were used.
(16) G. Herzberg, "Electronic Spectra of Polyatomic Molecules", Van Nostrand-Reinhold, Princeton, N.J., 1966.
(17) W. S. Benedict, N. Gailar, and E. K. Plyler, *J. Chem. Phys.*, **24**, 1139 (1956).
(18) One might be concerned about quasi-ionic (i.e., $r^{-1}$) effects at large separations. However, with the best fit parameters, there is almost complete cancellation among the $r^{-1}$ terms at long range. Also, we never calculate energies when $R_{CO} > 8.9$ Å.
(19) G. N. Sarkisov, V. G. Dashevsky, and G. G. Malenkov, *Mol. Phys.*, **27**, 1249 (1974).
(20) W. L. Masterton, *J. Chem. Phys.*, **22**, 1830 (1954).
(21) V. G. Dashevsky and G. N. Sarkisov, *Mol. Phys.*, **27**, 1271 (1974).
(22) We had hoped to calculate the free energy of hydration of methane by a non-Boltzmann sampling technique that we have developed (J. C. Owicki and H. A. Scheraga, *J. Phys. Chem.*, submitted for publication), but the slow water structural relaxation rendered this computationally unfeasible.

# A Modification of the Hückel Rule. Effective Discontinuity of Cyclic Conjugation

**Satoshi Inagaki* and Yoshio Hirabayashi**

*Contribution from the Department of Synthetic Chemistry, Faculty of Engineering, Gifu University, Kakamigahara, Gifu 504, Japan.* *Received August 27, 1976*

**Abstract:** The degree of cyclic electron delocalization is theoretically proposed in an unequivocal manner to be a function of mode of donor (D)–acceptor (A) arrangements of component systems as well as orbital phase continuity requirements. Cyclic conjugation is continuous only for such a D–A arrangement mode as **11**, to which the orbital phase continuity requirements or the Hückel rule contained in them are applicable. Cyclic conjugation is so effectively discontinuous for **12, 13,** etc., that the orbital phase relation makes no essential sense. There are nondelocalized $4n + 2$ $\pi$ electron (or nonaromatic) systems and nonlocalized $4n$ $\pi$ electron (or nonantiaromatic) systems in discontinuously conjugated systems. A novel notion of continuity–discontinuity of cyclic conjugation is exemplified by the experimental results, applied to interesting recent topics, and employed in predicting electronic properties of unknown molecules and in suggesting a device for synthesis of unstable molecules by varying substituents.

"Aromatic" chemistry has long been one of the most fascinating spheres of organic chemistry where both theoreticians and synthesists cooperated with fruitful results.[1,2] Among the theories the Hückel rule[1] is always overwhelmingly important because of its simplicity and wide coverage while other definitions of aromaticity have been proposed in various ways.[2m,n] It is, however, natural that the coverage of the dichotomy based on the number of electrons should be limited. Molecular properties continuously change from one molecule to another in the spectra of which the extremes are $4n + 2$ $\pi$ electron aromatic and $4n$ $\pi$ electron antiaromatic systems. It would be interesting to ask whether or not there are any other criteria on which the further detailed nature of cyclic conjugation is predicted or explained.

Essential factors underlying the Hückel rule are disclosed in this paper. Degree of cyclic electron delocalization depends on mode of donor (D)–acceptor (A) arrangements as well as the orbital phase continuity. The condition on which the criterion based on the number of electrons becomes invalid is presented in an unequivocal manner. The theoretical conclusions are exemplified by available experimental results. Application is also made to recent interesting topics, in some cases, together with prediction.

## Theoretical Background

The cyclic electron delocalization condition of three interacting systems has been derived from the third-order perturbation energy.[3,4] This is finally expressed in terms of the sign (+ or −) of product of three electron configuration or orbital overlap integrals. The configurations of interest are the initial configuration and the two important transferred configurations inferred from the relative D–A property. The delocalization condition was previously applied to a variety of chemical problems, i.e., catalytic reactions caused by transition metal complexes,[3] a classification of bicyclic compounds with $\pi$ bonds on each bridge as electron-delocalizing, semi-electron-delocalizing, and electron-localizing systems,[4] etc.

The physical meaning of the formalism and the successful application allow us to suppose that electron delocalization among many ($n$) systems is formally described by the $n$th order perturbation energy, or by the sign of product of $n$ configuration overlaps

$$S_{IJ}S_{JK}\ldots S_{ZI} > 0 \qquad (1)$$

where the subscript $I$ is the initial configuration, others being important transferred configurations. The similarity of the inequality seems to lead without any proviso to the same orbital phase continuity requirements as those for three-system interaction: (1) the HOMO's of the neighboring systems should be out of phase; (2) the LUMO's of the neighboring systems should be in phase; (3) the HOMO and the LUMO of the neighboring systems should be in phase. It is readily seen that these requirements contain the Hückel rule. However, favorable D–A arrangements are found to be prerequisite to the validity for more than three systems.

It may be helpful to summarize the general results obtained from the previous studies on the three-system interaction.[3,4] (1) Electron delocalization is described in terms of interactions between the initial configuration and transferred configurations and between transferred configurations. (2) The interaction between the initial and the transferred configurations, $D_i \rightarrow A_j$, is effective only when the transferred configuration involves an electron shift between a neighboring D–A pair (**1**). The interaction corresponds to the electron delocalization